ATLASGAL – Complete compact source catalogue: 280° < ℓ < 60°[⋆]
(Research Note)

J. S. Urquhart[1], T. Csengeri[1], F. Wyrowski[1], F. Schuller[1,2], S. Bontemps[3], L. Bronfman[4], K. M. Menten[1],
C. M. Walmsley[5,6], Y. Contreras[7], H. Beuther[8], M. Wienen[1], and H. Linz[8]

[1] Max-Planck-Institut für Radioastronomie, Auf dem Hügel 69, Bonn, Germany
e-mail: jurquhart@mpifr-bonn.mpg.de
[2] European Southern Observatory, Alonso de Cordova 3107, Vitacura, Santiago, Chile
[3] Laboratoire d'Astrophysique de Bordeaux – UMR 5804, CNRS, Université Bordeaux 1, BP 89, 33270 Floirac, France
[4] Departamento de Astronomía, Universidad de Chile, Casilla 36-D, Santiago, Chile
[5] Osservatorio Astrofisico di Arcetri, Largo E. Fermi 5, 50125 Firenze, Italy
[6] Dublin Institute for Advanced Studies, 31 Fitzwilliam Place, Dublin 2, Ireland
[7] CSIRO Astronomy and Space Science, PO Box 76, Epping, NSW 1710, Australia
[8] Max-Planck-Institut für Astronomie, Königstuhl 17, 69117 Heidelberg, Germany

ABSTRACT

Context. The APEX Telescope Large Area Survey of the Galaxy (ATLASGAL) is the largest and most sensitive systematic survey of the inner Galactic plane in the submillimetre wavelength regime. The observations were carried out with the Large APEX Bolometer Camera (LABOCA), an array of 295 bolometers observing at 870 μm (345 GHz).
Aims. In this research note we present the compact source catalogue for the 280° < ℓ < 330° and 21° < ℓ < 60° regions of this survey.
Methods. The construction of this catalogue was made with the source extraction routine SExtractor using the same input parameters and procedures as used to analyse the inner Galaxy region presented in an earlier publication (i.e., 330° < ℓ < 21°).
Results. We have identified 3523 compact sources and present a catalogue of their properties. When combined with the regions already published, this provides a comprehensive and unbiased database of ∼10 163 massive, dense clumps located across the inner Galaxy.

Key words. stars: formation – surveys – submillimeter: ISM – catalogs

1. Introduction

The APEX Telescope Large Area Survey of the Galaxy (ATLASGAL) is an unbiased 870 μm submillimetre survey covering 420 sq. degrees of the inner Galactic plane (Schuller et al. 2009). The regions covered by this survey are |ℓ| < 60° with |b| < 1.5° and 280° < ℓ < 300° with b between −2° and 1°; the change in latitude was necessary to account for the warp in the Galactic disc in the outer Galaxy extension. The thermal emission from dust is optically thin at submillimetre wavelengths and contribution from free-free emission should be negligible, making it an excellent tracer of column density and total clump mass. The fundamental goal of ATLASGAL is to provide a large and systematic inventory of massive, dense clumps in the Galaxy that includes representative samples of all of the earliest embedded stages of high-mass star formation.

ATLASGAL is the largest and most sensitive submillimetre ground-based survey that covers approximately two-thirds of the surface area of the Galactic molecular disc within ∼15 kpc of the Galactic centre (see Fig. 1 for a schematic of survey coverage). This increases to almost 100% of the surface area of the molecular disc within the solar circle (i.e., R_{gc} < 8.5 kpc) and includes all of the 5 kpc molecular ring where the majority

of the molecular gas in the Galaxy resides (i.e., 4 < R_{gc} < 6 kpc; Stecker et al. 1975). This survey has a sensitivity of 0.3−0.5 Jy beam^{-1} (5σ; see Sect. 2 for details) and is able to detect all cold dense clumps (<25 K) with masses ≥1000 $M_\odot$ at a heliocentric distance of 20 kpc, which is sufficient to find all massive star forming clumps located in the inner Galaxy (assuming a standard initial mass function and a typical star formation efficiency; Urquhart et al. 2013a). Furthermore, this survey complements many of the other Galactic plane surveys: e.g., UKIDSS (Lucas et al. 2008), GLIMPSE (Benjamin et al. 2003), *Herschel* Hi-GAL (Molinari et al. 2010), Bolocam Galactic Plane Survey (Aguirre et al. 2011), and the Co-ordinated Radio and Infrared Survey for High-Mass Star Formation (CORNISH; Purcell et al. 2013 and Hoare et al. 2012).

To date, two methods have been used to identify sources present in the ATLASGAL emission maps and extract their parameters. The first method used was the SExtractor extraction algorithm (Bertin & Arnouts 1996) that was applied to a ∼150 sq. degree region located towards the Galactic centre (i.e., 330° < ℓ < 21°; Contreras et al. 2013). This method is sensitive to the large-scale structures of dense clumps and small molecular clouds, and it identified 6640 sources above a threshold of 3σ (∼180−300 mJy beam^{-1}) and is 99% complete above 6σ. The second method consists of a two-step process where the emission maps are first filtered to remove the large-scale diffuse structure, and then the GaussClump algorithm is used to identify and
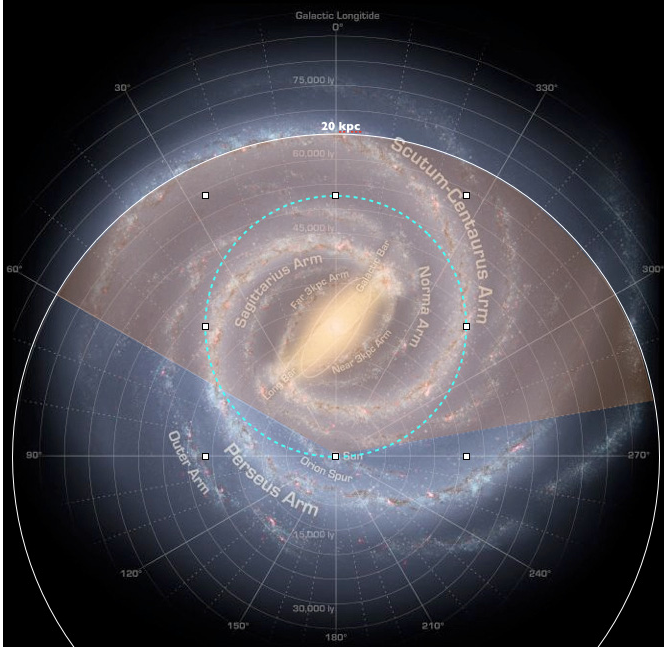

Fig. 1. Schematic of the Galaxy showing the region covered by ATLASGAL. The background image is an artist impression of the Galactic plane, and it incorporates much of what is known about the large-scale structure of the Galaxy and shows the location of the spiral arms and the Galactic bar. The solar circle is shown in by the dashed cyan line and the region of the Galaxy covered by the ATLASGAL survey shown by the light brown shading. Background image courtesy of NASA/JPL-Caltech/R. Hurt (SSC/Caltech).

extract source parameters by fitting a 2D Gaussian to the structures. This method has been applied to the whole ATLASGAL survey region (i.e., $280° < \ell < 60°$) and has identified almost 11 000 compact embedded objects above a more conservative 5σ threshold (Csengeri et al. 2014).

We refer to the `SExtractor` and `GaussClump` catalogues as the Compact Source Catalogue (CSC) and GaussClump Source Catalogue (GCSC), respectively[1]. The two methods have been designed to be sensitive to different structures with the former providing information on the global parameters of the whole clump, while the latter is better for estimating the properties of the gas more closely associated with the star formation process (see Sect. 3 for more details).

In this research note, we present the results of the `SExtractor` source extraction for the region not covered by Contreras et al. (2013). A detailed description of the survey is provided by Schuller et al. (2009) and a comprehensive discussion of the `SExtractor` algorithm, procedures used, catalogue completeness, and reliability tests can be found in Contreras et al. (2013). We provide only a brief summary of the ATLASGAL survey and the source extraction method in Sect. 2 and refer the reader to the these two papers for more details. In Sect. 3 we present the catalogue of new sources and compare their properties with those identified by Contreras et al. (2013) and with the GCSC (Csengeri et al. 2014). We present a summary and outlook in Sect. 4.

---

[1] http://atlasgal.mpifr-bonn.mpg.de/cgi-bin/ATLASGAL_DATABASE.cgi

2. Survey and source extraction summary

The observations were carried out with the APEX (Atacama Pathfinder EXperiment) 12 m submillimetre telescope (Güsten et al. 2006), located in Llano de Chajnantor, Chile. The Large APEX BOlometer CAmera (LABOCA; Siringo et al. 2009) was used to map the $870\,\mu$m emission across the inner Galaxy. The instrument bandpass is centred at 345 GHz and has a bandwidth of 60 GHz, which corresponds to FWHM beam size of $19\rlap{.}''2$. The typical pointing rms error is $\sim4''$. The noise varies between 60 and 100 mJy beam^{-1} across the survey region depending on the number of coverages, the atmospheric conditions at the time of the observations and telescope elevation. The lower values are typically found towards the Galactic centre regions, and the highest values are associated with the extension region (i.e., $280° < \ell < 300°$; see Fig. 1 of Csengeri et al. 2014).

`SExtractor` was used to identify coherent emission in the signal-to-noise ratio (S/N) maps above a threshold value of 3 and associated with more pixels than the beam integral (i.e., ~11 pixels). We have used the same input parameters and emission maps reduced in the same way as those used by Contreras et al. (2013) and therefore represents a natural extension to their work and combine provides a fully consistent catalogue covering the whole ATLASGAL survey. The S/N maps were produced by dividing the emission maps by the square root of the weight maps. Using them avoids problems encountered when trying to identify sources using a flux threshold in fields where the background noise is varying. The parameters of the sources above the threshold are then extracted from the original emission maps.

Tests were performed to check the reliability of the `SExtractor` algorithm and the catalogue of extracted sources. This was done by injecting artificial sources into two types of synthetic maps: one where the noise properties were Gaussian and another where the noise included a varying component introduced to better reflect the diffuse emission seen in the survey emission maps. `SExtractor` recovered 99% of injected sources in both types of maps above a threshold of $\sim6\sigma$ and this is taken as the completeness of the catalogue and as reliable detections (for more details see Sect. 4 of Contreras et al. 2013).

3. Compact source catalogue

3.1. Catalogue description

We ran `SExtractor` on thirty $3° \times 3°$ fields outside the region previously reported by Contreras et al. 2013 (i.e., $280° < \ell < 330°$ and $21° < \ell < 60°$) and identified a further 3523 compact sources in this 267 sq. degree region. In Table 1 we present a sample of the catalogue as an example of its form and content. In this table we present the source name, the positions of the emission peak and its geometric centre, the size of the semi-major and minor axis and their position angle, the deconvolved radius, the peak and integrated fluxes and their associated errors, and any warning flags generated by the algorithm identify possible problems or artefacts affecting the source.

The deconvolved source sizes are estimated assuming Gaussian beam characteristics following Rosolowsky et al. (2010) such that

$$\theta_R = \eta \left[(\sigma_{\mathrm{maj}}^2 - \sigma_{\mathrm{bm}}^2)(\sigma_{\mathrm{min}}^2 - \sigma_{\mathrm{bm}}^2) \right]^{1/4}, \tag{1}$$

where σ_{bm} is the 1σ Gaussian beam size (i.e., $\sigma_{\mathrm{bm}} = \theta_{\mathrm{FWHM}}/\sqrt{8\ln 2} \simeq 8''$) and a value for η of 2.4 (Rosolowsky et al. 2010) that relates the measured size to the source's effective radius (i.e., $R_{\mathrm{eff}} = \sqrt{(A/\pi)}$, where A is the surface area

Table 1. ATLASGAL compact source catalogue for sources located in the $280° < \ell < 330°$ and $21° < \ell < 60°$ region.

Catalogue name (1)	ℓ_{max} (°) (2)	b_{max} (°) (3)	ℓ (°) (4)	b (°) (5)	σ_{maj} (″) (6)	σ_{min} (″) (7)	PA (°) (8)	θ_R (″) (9)	S_{peak} (Jy beam^{-1}) (10)	ΔS_{peak} (11)	S_{int} (Jy) (12)	ΔS_{int} (13)	Flag (14)	S/N (15)
AGAL300.164−00.087	300.164	−0.087	300.164	−0.089	11	7	10	⋯	1.39	0.26	5.09	1.02	0	8.9
AGAL300.218−00.111	300.218	−0.111	300.218	−0.113	19	12	122	30	1.17	0.26	5.68	1.11	0	6.2
AGAL300.323−00.199	300.323	−0.199	300.323	−0.199	8	6	138	⋯	0.71	0.38	2.28	0.57	16	1.9
AGAL300.341−00.214	300.341	−0.214	300.340	−0.213	13	9	140	16	0.76	0.30	5.30	1.05	2	2.7
AGAL300.381−00.287	300.381	−0.287	300.379	−0.286	25	13	141	37	0.90	0.14	7.11	1.33	0	97.4
AGAL300.403+00.544	300.403	0.544	300.404	0.544	13	10	129	19	1.02	0.61	3.38	0.75	0	1.7
AGAL300.456−00.189	300.456	−0.189	300.455	−0.191	14	9	15	17	0.94	0.17	4.29	0.89	0	9.9
AGAL300.491−00.176	300.491	−0.176	300.489	−0.175	20	12	172	31	0.68	0.15	6.12	1.18	3	6.5
AGAL300.499−00.212	300.499	−0.212	300.500	−0.211	17	7	7	⋯	0.58	0.12	2.52	0.61	3	6.5

Notes. The columns are as follows: (1) name derived from Galactic coordinates of the maximum intensity in the source; (2)−(3) Galactic coordinates of maximum intensity in the catalogue source; (4)−(5) Galactic coordinates of emission centroid; (6)−(8) semi-major and semi-minor size and source position angle measured anti-clockwise from Galactic north; (9) effective radius of source; (10)−(13) peak and integrated flux densities and their associated uncertainties; (14) SExtractor detection flag (see Bertin & Arnouts 1996 notes on these flags); (15) signal-to-noise ratio (S/N) – values for sources with peak flux below 6σ detection should not be used blindly. Only a small portion of the data is provided here, the full table is only available in electronic form at the CDS.
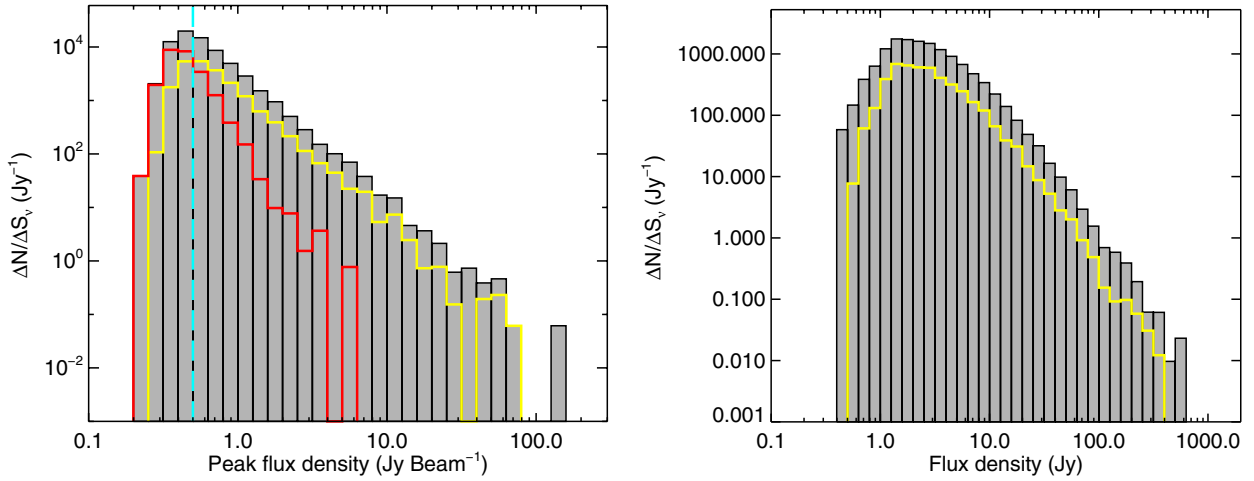

Fig. 2. Flux density distribution for the full ATLASGAL CSC extracted by SExtractor (grey filled histogram) and the sources located in the $280° < \ell < 330°$ and $21° < \ell < 60°$ region (yellow). In the *left and right panels* we present histograms of the peak and integrated flux densities measured for each source, respectively. The dashed vertical lines shown in the *left panel* indicate the nominal 6σ sensitivity range above which the catalogue is considered complete (i.e., $0.3-0.5$ Jy beam^{-1}). The red histogram shows the peak flux distribution of sources not matched with a source identified by the GaussClump catalogue. The bin width is 0.1 dex.

of the source; Dunham et al. 2011). An important caveat is that since the source sizes are determined only using the pixels above the detection threshold, we are likely to underestimate the true source sizes, and in some cases this can result in source sizes that are smaller than the beam.

The errors given for the peak and integrated fluxes include the absolute calibration uncertainty of 15% and the intrinsic measurement error, which are added in quadrature. In Col. 14 we give the quality flag provided by SExtractor, which identifies possible problems or artefacts affecting the source (see Bertin & Arnouts 1996 for details) and in the final column we give the S/N for each source.

3.2. Catalogue properties

Combined with the sources previously identified from analysis of the $330° < \ell < 21°$ region reported by Contreras et al. (2013), the complete ATLASGAL CSC consists of 10 163 sources. In Fig. 2 we present plots showing the peak and integrated flux densities for the full CSC catalogue and for comparison the new sources reported here. The slopes of the two distributions are very similar and a power-law fit to the bins above the turnover (~ 0.5 Jy beam^{-1}; corresponds to the nominal completeness) finds slopes of -2.43 ± 0.04 and -2.41 ± 0.07 for the full catalogue and new sources, respectively. The peak flux distributions are therefore in excellent agreement with each other and the value reported by Contreras et al. (2013) for the inner Galaxy region (i.e., -2.4 ± 0.04). Analysis of the integrated flux distribution finds similar agreement between the full CSC and the sources reported here and by Contreras et al. (2013). We therefore conclude that there are no systematic differences in the flux properties of the whole SExtractor catalogue.

In Fig. 3 we present a cumulative distribution plot showing the measured aspect ratio of the full catalogue (i.e., $\theta_{maj}/\theta_{min}$) and the Contreras et al. (2013) subsample and the new sources reported here. Inspection of these distributions reveals the new sources have slightly smaller aspect ratios than the Contreras et al. (2013) subsample (a Kolmogorov-Smirnov test finds this
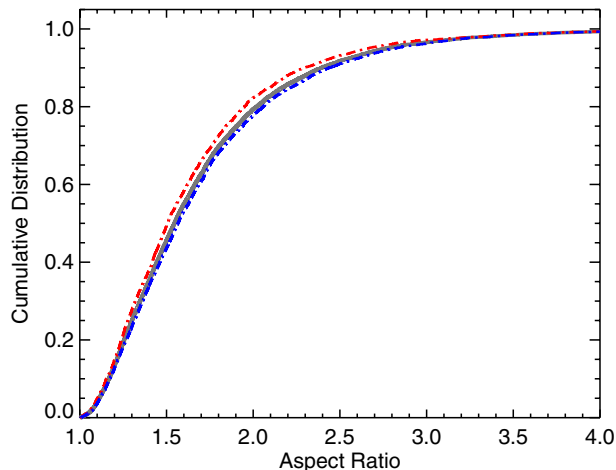
Fig. 3. Cumulative distributions of the aspect ratio for the full ATLASGAL CSC (grey curve) and the sources reported here and by Contreras et al. (2013) are shown by the red and blue curves, respectively.

difference is significant with a probability ≪0.01 that the two samples are drawn from the same parent distribution, i.e., less than 3σ). However, the source density in the $280° < \ell < 330°$ and $21° < \ell < 60°$ regions is significantly lower and the overall emission is less complicated, and there is less blending of sources, which is likely to result in more elongated sources being found towards the innermost part of the Galactic plane.

3.2.1. Comparison with the GaussClump catalogue

A comparison between the two catalogues is presented by Csengeri et al. (2014), so we only present a brief summary and discuss a few points not mentioned previously. Both catalogues contain a similar number of sources with 10 163 identified by SExtractor and 10 861 identified by GaussClumps (Csengeri et al. 2014), however, only approximately 7600 CSC and 10 400 GCSC sources are common to both catalogues, with ~1600 CSC sources being associated with 2 or more GCSC sources (see Fig. 4 for an example). There are ~500 GCSC sources without a counterpart in the CSC; however, in the majority of cases (90%) a source was detected by SExtractor, but these were later excluded as they had fewer than 11 pixels. There are some ~2500 CSC sources without GCSC counterparts, but the majority of them fall below the 5σ threshold required for inclusion in that catalogue. In the lefthand panel of Fig. 2 we show the flux distribution of CSC sources without a GCSC counterpart that shows the unmatched sources dominate the lower peak flux density part of the distribution. The remaining unmatched CSC sources found are more extended regions of emission that were removed by the large-scale filtering in the GCSC catalogue.

The differences noted here nicely illustrate the complementary strengths of the two catalogues with the CSC providing a more global distribution of the dust, while the GCSC has better sensitive to even more compact sources (as illustrated in Fig. 4).

4. Summary

The ATLASGAL has mapped $420 \deg^2$ of the inner Galaxy at $870\,\mu m$, which traces thermal emission from dense clumps. In this research note we present analysis of ~270 sq. degrees not included in the previous Compact Source Catalogue (CSC; Contreras et al. 2013). This analysis identified an additional 3523 compact sources located within the $280° < \ell < 330°$ and
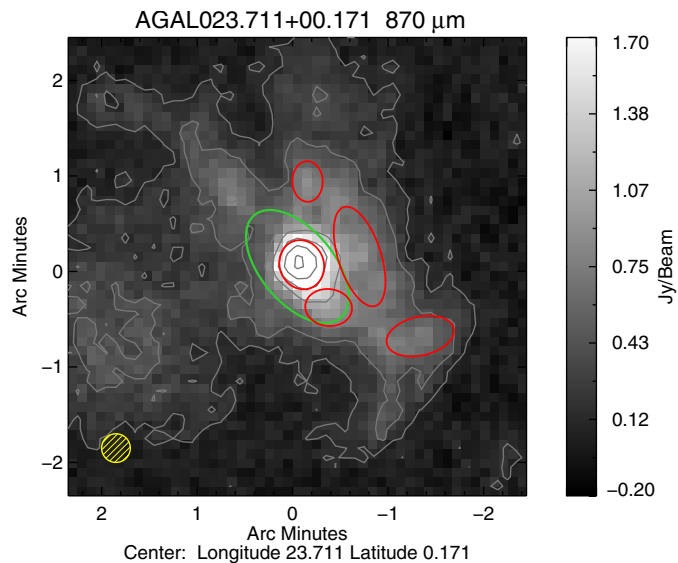

Fig. 4. Example of a source detected by both extraction algorithms but where GaussClump has separated the emission into multiple components. The greyscale shows the ATLASGAL dust emission and the red hatched circle shown in the lower left corner indicates the APEX FWHM beam size. The position and size of the CSC source is indicated by the green ellipse and the multiple GCSC sources are indicated by the yellow ellipses. Contours start and increase in steps of 3σ.

$21° < \ell < 60°$ regions of the Galactic disc. Combined with the catalogue presented by Contreras et al. (2013), the full CSC now consists of 10 163 compact sources and provides a complete inventory of massive star forming clumps with masses $\geq 1000\,M_\odot$ within the inner Galactic plane, as well as large, but less complete, samples of lower mass clumps. This catalogue has already been used to identify large samples of massive star forming clumps and investigate their properties (i.e., Urquhart et al. 2013a,b, 2014) and will be an indispensable resource for future studies with ALMA[1].

References

Aguirre, J. E., Ginsburg, A. G., Dunham, M. K., et al. 2011, ApJS, 192, 4
Benjamin, R. A., Churchwell, E., Babler, B. L., et al. 2003, PASP, 115, 953
Bertin, E., & Arnouts, S. 1996, A&AS, 117, 393
Contreras, Y., Schuller, F., Urquhart, J. S., et al. 2013, A&A, 549, A45
Csengeri, T., Urquhart, J. S., Schuller, F., et al. 2014, A&A, 565, A75
Dunham, M. K., Robitaille, T. P., Evans, II, N. J., et al. 2011, ApJ, 731, 90
Güsten, R., Nyman, L. Å., Schilke, P., et al. 2006, A&A, 454, L13
Hoare, M. G., Purcell, C. R., Churchwell, E. B., et al. 2012, PASP, 124, 939
Lucas, P. W., Hoare, M. G., Longmore, A., et al. 2008, MNRAS, 391, 136
Molinari, S., Swinyard, B., Bally, J., et al. 2010, PASP, 122, 314
Purcell, C. R., Hoare, M. G., Cotton, W. D., et al. 2013, ApJS, 205, 1
Rosolowsky, E., Dunham, M. K., Ginsburg, A., et al. 2010, ApJS, 188, 123
Schuller, F., Menten, K. M., Contreras, Y., Wyrowski, F., & Schilke, E. A. 2009, A&A, 504, 415
Siringo, G., Kreysa, E., Kovács, A., et al. 2009, A&A, 497, 945
Stecker, F. W., Solomon, P. M., Scoville, N. Z., & Ryter, C. E. 1975, ApJ, 201, 90
Urquhart, J. S., Moore, T. J. T., Schuller, F., et al. 2013a, MNRAS, 431, 1752
Urquhart, J. S., Thompson, M. A., Moore, T. J. T., et al. 2013b, MNRAS, 435, 400
Urquhart, J. S., Moore, T. J. T., Csengeri, T., et al. 2014, MNRAS, 443, 1555